Lawrence Berkeley National Laboratory
LBL Publications

**Title**

STRUCTURE DETERMINATION OP THE PLATINUM (111) CRYSTAL FACE BY LOW-ENERGY ELECTRON DIFFRACTION

**Permalink**

https://escholarship.org/uc/item/4hj9z8fz

**Authors**

Kesmodel, L. L.
Somorjai, G.A.

**Publication Date**

1974-08-01

eScholarship.org Powered by the California Digital Library
University of California

Submitted to ~~Journal~~ Physical Review

LBL-3148
Preprint c.2

# STRUCTURE DETERMINATION OF THE PLATINUM (111) CRYSTAL FACE BY LOW-ENERGY ELECTRON DIFFRACTION

L. L. Kesmodel and G. A. Somorjai

August, 1974

Prepared for the U. S. Atomic Energy Commission
under Contract W-7405-ENG-48

TWO-WEEK LOAN COPY

*This is a Library Circulating Copy which may be borrowed for two weeks. For a personal retention copy, call Tech. Info. Division, Ext. 5545*

LAWRENCE BERKELEY LABORATORY
UNIVERSITY OF CALIFORNIA BERKELEY

LBL-3148 c.2

# DISCLAIMER

This document was prepared as an account of work sponsored by the United States Government. While this document is believed to contain correct information, neither the United States Government nor any agency thereof, nor the Regents of the University of California, nor any of their employees, makes any warranty, express or implied, or assumes any legal responsibility for the accuracy, completeness, or usefulness of any information, apparatus, product, or process disclosed, or represents that its use would not infringe privately owned rights. Reference herein to any specific commercial product, process, or service by its trade name, trademark, manufacturer, or otherwise, does not necessarily constitute or imply its endorsement, recommendation, or favoring by the United States Government or any agency thereof, or the Regents of the University of California. The views and opinions of authors expressed herein do not necessarily state or reflect those of the United States Government or any agency thereof or the Regents of the University of California.

# STRUCTURE DETERMINATION OF THE PLATINUM (111) CRYSTAL FACE BY LOW-ENERGY ELECTRON DIFFRACTION

L. L. Kesmodel and G. A. Somorjai

Department of Chemistry, University of California
and Inorganic Materials Research Division, Lawrence Berkeley Laboratory
Berkeley, California 94720

## ABSTRACT

An analysis of low-energy electron diffraction intensity profiles from the clean (111) face of platinum is carried out. Calculated intensities are compared with experimental results for specular and non-specular beams at several angles of incidence for electron energies $\leq$100 eV. The calculations are based on a T-matrix multiple-scattering theory with corrections for lattice vibrations. The scattering from a single atomic site is modeled with a conventional band structure potential parameterized by six partial-wave phase shifts. The constant inner potential $V_0$ determined from addition of the Fermi energy and a measured value of the work function is found to predict the peak positions accurately. The calculations adequately describe the shapes and relative intensities of primary and secondary features in the experimental intensity profiles. Analysis of the data indicates that the spacing of the topmost atomic layer is the same as the bulk value to within 5% (or approximately 0.1Å).

## I. INTRODUCTION

In the preceding paper, Stair, Kaminska and the present authors have presented low-energy electron diffraction intensity vs. voltage (I-V) profiles for the (111) face of clean platinum in the energy range 20-200 eV by both photometric and photographic experimental techniques.[1] In this paper a multiple-scattering theory of low-energy electron diffraction is applied to the analysis of the data and conclusions are drawn as to the structure of the clean Pt(111) surface. We regard these results as significant in two general respects. Firstly, there is great current interest in understanding the structures of adsorbed overlayers of various molecules on platinum because of its important catalytic properties. The demonstration of the applicability of low-energy electron diffraction theory to the determination of the structure of the clean platinum surface is a first step toward this goal. Secondly, these results are the first that are reported for a 5d transition metal and indicate that the theoretical models used successfully for the lighter elements are applicable to the heavier, strong-scattering elements. Our results on platinum taken together with previous work on aluminum,[2-5] nickel,[6-8] copper,[2,9-11] and silver[2,12] argue for the validity of the rather simple theoretical models used to describe the scattering of the low-energy electrons from the clean faces of transition and noble metals as well as the more free-electron-like metals.

The central components of the theory of elastic low-energy electron diffraction from solid surfaces are a description of multiple-scattering processes, the inclusion of reasonable atomic scattering potentials, and an approximate treatment of the effects of inelastic scattering on the elastic electron beam. Moreover, refined models should have some provision for the effects of lattice vibrations and may also include a treatment of the scattering of the electrons from the vacuum-solid barrier potential. Of course, all of these components may be only approximately accounted for, and, therefore, the underlying assumption in all such model analyses is that the lattice geometry itself is the dominant parameter in the diffraction process. This assumption has been borne out by the general success of low-energy electron diffraction model calculations in the past few years. In the present work, we apply a T-matrix multiple scattering theory[13-15] to the structure analysis of the Pt(111) surface. The calculations employ the computer program used earlier by Tong and Kesmodel.[7] As discussed below, the model calculations are carried out using a conventional band structure potential and a simple treatment of the inner potential. An effort was made in this work to give an accurate numerical calculation within the framework of the model parameters. In this way, differences between experimental and calculated I-V profiles are directly attributable to inaccuracies in the model itself. In particular, we found that six partial wave phase shifts were necessary to give an accurate description of the platinum atomic scattering factor for energies 50-100 eV above the vacuum and that a larger number of phase shifts would be necessary above 100 eV. In order to achieve numerical accuracy and at the same time fall within computer core size and time limitations we restricted the calculations to the energy range $20 \text{ eV} \leq E \leq 100 \text{ eV}$ and used six partial wave phase shifts. Comparisons between calculated and experimental I-V profiles indicates overall agreement within 2 eV in peak positions and adequate agreement in relative peak heights and peak shapes. Analysis of the data indicates that the upper layer spacing for Pt(111) is the same as the bulk value to within 5% (or approximately 0.1Å).

## II. OUTLINE OF THE THEORETICAL MODEL

The theoretical model used in this work for calculating the I-V profiles from platinum has been used previously by the present authors as well as by Duke, Laramore, and co-workers and Tong and co-workers. The formalism is based on an exact multiple scattering method originally proposed by Beeby.[13] The theory was subsequently modified to include inelastic-collision damping by Duke and Tucker[14] and the approximate effects of lattice vibrations by Duke and Laramore.[15] The details of our method have been outlined in a recent paper on nickel by Tong and Kesmodel[7] and references contained therein. The reader is also referred to Refs. 18-19 for a general review of low-energy electron diffraction theory as well as experimentation. In this section, we discuss those features of the model relevant to the scattering from platinum.

Of fundamental importance is the atomic scattering potential that describes the scattering of the electron by a single atomic site. Previous work on clean metal surfaces has indicated that conventional band structure potentials constructed for electrons near the Fermi energy of the solid also work adequately for the higher energies relevant to low-energy electron diffraction. In this work we used the muffin-tin potential constructed by Andersen and Mackintosh [16] in their relativistic-augmented-plane-wave (RAPW) band structure calculation on platinum. Their calculation employed the Slater[17] free-electron approximation for the exchange in its full strength. The potential was not self-consistent but its accuracy was rather judged by the agreement with Fermi-surface dimensions and velocities. The calculation used a lattice constant of 3.92Å and a muffin-tin radius of 1.37Å. The

Fermi energy was calculated to be 8.9 eV above the constant value of the potential between muffin-tin spheres (the muffin-tin zero (MTO)). We use the so-called "no-reflection" boundary condition on the incident and outgoing electron, meaning that we consider the surface barrier potential to smoothly accelerate the electron in the direction normal to the surface, and we do not consider reflections from the barrier itself. This approximation has been discussed in several earlier treatments and has shown to be valid for energies greater than about 20 eV above the vacuum level. Therefore, the main effect of the barrier in this treatment is to shift the energy of the electron in solid by an inner potential, $V_o$, above its energy in vacuum. The value of the inner potential, $V_o$, used in the calculations herein was simply taken to be the sum of the Fermi energy and the measured value of 5.4 eV for the platinum work function,[20] giving $V_o = 14.3$ eV. Strictly speaking this value of $V_o$ is only appropriate for an electron near the Fermi energy since the exchange-correlation part of the vacuum-solid barrier potential seen by an electron is in general energy dependent. One may also consider an effective energy dependence in the parameter $V_o$ due to depth dependence in the inner potential. However, as discussed below in Sec. III, we find the constant value of $V_o$ determined above to give an excellent description of the peak positions in the I-V profiles within the anticipated error of about 2 eV attendant with low-energy electron diffraction theory.

The phase shifts calculated from the spherically symmetric muffin-tin potential are shown in Figure 1 in the energy range 0-180 eV above the MTO.

Platinum is a strong scatterer and we note that the $\ell = 0\text{-}4$ phase shifts are quite strong for most energies and the $\ell = 5,6$ phase shifts become significant at the higher energies. The total elastic scattering cross section calculated from these phase shifts is fairly constant throughout the energy range 15-200 eV above vacuum, having a maximum value of $9.7\text{Å}^2$ at 45 eV. This area is to be compared with the cross-sectional area of $6.6\text{Å}^2$ of the unit mesh of the densely packed (111) planes of platinum. The atomic scattering factor $f(\theta)$ given by the formula[21]

$$f(\theta) = \frac{1}{k} \sum_{\ell=0}^{\infty} (2\ell + 1) e^{i\delta_\ell(k)} \sin\delta_\ell(k)\, P_\ell(\cos\theta) \qquad (1)$$

describes the dependence of the scattering at energy E from a single atomic site on the scattering angle $\theta$ from the forward direction. Here $k = \sqrt{2mE/\hbar^2}$, the $\delta_\ell$ are the phase shifts and the $P_\ell$ are the Legendre polynomials. The modulus of the atomic scattering factor for platinum at 100 eV above the vacuum level is shown as a function of the scattering angle in Figure 2. The series in Equation (1) is essentially converged after six phase shifts ($\ell = 0, \ldots, 5$) for $E \lesssim 100$ eV but the neglect of the $\ell = 5$ phase shift leads to significant differences in the angular structure of $f(\theta)$ for $E \gtrsim 50$ eV. Although these differences are primarily in the part of the curve $40° \lesssim \theta \lesssim 180°$ where $f(\theta)$ is relatively small, they will, of course, influence the back-scattering contribution to the intensity profiles. Indeed, trial calculations have indicated that the use of only five phase shifts causes significant errors in I-V peak intensities for $E \gtrsim 50$ eV and leads to major differences in peak positions for $E \gtrsim 90$ eV. As would be expected, these errors are most pronounced for the (00) beam at near-normal incidence where the single-scattering contribution comes from $\theta \simeq 180^\circ$ scattering. In order to allow a precise description of the model scattering factor and keep computer requirements manageable it was decided to restrict the calculation to energies $E \lesssim 100$ eV and use six partial wave phase shifts. This is not a drawback since the data is available on both specular and non-specular beams at four angles of incidence. Moreover, this is the energy range in which low-energy electrons are most sensitive to the surface region.

Finally, we mention the remaining parameters in the calculation dealing with the inelastic damping and the lattice vibrations. The value of the electron damping as parameterized by the imaginary part of the electron self-energy is generally taken to be 3-5 eV in the energy range of interest. We found that a constant value of 4 eV for this damping parameter gave a good description of peak widths and secondary features in the I-V profiles. Fortunately, the peak positions are rather insensitive to the value of the damping parameter. With the chosen value of the damping the intensity calculations were well-converged using five atomic layers, the bulk interlayer spacing being $d = 2.26$Å for the Pt(111) planes.

The correction to the intensity profiles due to the finite-temperature phonon scattering was accounted for by the Debye-Waller renormalization discussed previously by Duke and Laramore.[15] The magnitude of this correction in a kinematic model may be parameterized in terms of the temperature, the energy, the atomic mass, and the Debye temperature $\theta_D$. Using the platinum bulk Debye temperature of 234°K[22] one estimates the room-temperature Debye-Waller correction to reduce the rigid lattice scattering by approximately 20% at $E = 100$ eV. This correction is small due to the large atomic mass of platinum. The lattice vibrations in the surface region are expected to differ considerably from the bulk vibrations but since the Debye-Waller factor using bulk lattice vibrations is small we do not expect changes in the surface vibrations to radically affect the intensity profiles at room temperature for energies less than 100 eV. For this reason, and for lack of detailed knowledge of the surface vibrations, we described the atomic layers parallel to the surface by a single (bulk) Debye temperature of $\theta_D = 234°K$.

## III. RESULTS AND DISCUSSION

In this section we compare the results of calculations of the I-V profiles for clean Pt(111) with the experimental data of Stair et al., Ref. 1. The comparison is made to photometric data for the specular beam intensities and to photographic data for the non-specular beams. As discussed in Ref. 1, differences between the sets of data obtained by the two methods are small. The calculated I-V profiles were obtained with a computer program constructed by Tong and Kesmodel[7] which solves the scattering equations by an exact matrix inversion procedure. Details of the method relevant to the scattering from platinum have been discussed in Sec. II. As discussed in Ref. 1, only relative intensities were measured, and no effort was made to relate the intensity scale from one beam to another.

The diffraction pattern from Pt(111) (Figure 3) has the hexagonal geometry expected from the simple termination of the bulk fcc structure in the direction perpendicular to the (111) planes. There is no evidence for a reconstruction as occurs, for example, in Pt(100) or Pt(110), but one may reasonably postulate the possible movement of the topmost or top few layers in the direction perpendicular to the surface. The symmetry of the diffraction pattern intensities at normal incidence is three-fold as follows from the ABC ABC ... close-packed stacking sequence, the (10) and (01) beams of Figure 3 being non-degenerate. The question, of course, arises as to the orientation of the spot pattern with respect to the two nonequivalent 60°-rotated orientations of the surface crystallographic unit cell. The orientation shown in Figure 3 was determined by intensity analysis of the non-specular beams and provides an unambiguous labelling of these beams.

The experimental and calculated I-V profiles for both specular and non-specular beams are shown in Figures 4-6. The calculations were made first assuming the bulk interlayer spacing of d = 2.26Å. The results for the (00) and $(\bar{1}0)$ beams at $\phi = 0°$, $\theta = 4°, 10°$ and $\phi = 4.3°$, $\theta = 16°$ are shown in Figure 4. The agreement in peak positions is excellent for both (00) and $(\bar{1}0)$ beams. There is also adequate agreement in relative peak intensities. Almost all of the secondary features of the experimental curves are brought out in the calculations. A notable example of this is the detailed structure in the I-V profile of the $(\bar{1}0)$ beam at $\theta = 10°$. The main discrepancies are in the relative intensities of some peaks in the (00) beam at $\theta = 10°$ and $\theta = 16°$. That is, the relative intensities of the doublet features occurring in the range 50-60 eV are not correctly reproduced in the theory. The results for the (10) and (01) beams at normal incidence are shown in Figure 5. Unfortunately, experimental measurements were not made of these beams just above their emergence energies and so the primary peaks occurring near 40 eV were not measured. The agreement for these beams is not as satisfactory as for the (00) and $(\bar{1}0)$ beams shown in Figure 4. The main discrepancy here is the shoulder peak occurring near 55 eV in both beams. This peak is absent in the theory except as a broad shoulder in the (01) beam calculation. However, the other peaks are adequately reproduced in the theory.

In order to make such comparisons more quantitative, a detailed tabulation of the experimental and calculated peak positions in the energy range $15 \leq E \leq 105$ eV is given for the (00) beam in Table 1 and for the non-specular beams in Table 2. An analysis of 28 peaks indicates the average error of $|\overline{\Delta}| = 1.6$ eV in calculated peak positions for the crystal surface having the bulk interlayer spacing and inner potential $V_0 = 14.3$ eV. We have also considered the possibility of a small expansion or contraction of the topmost atomic layer in the direction perpendicular to the surface. The "relaxed" layer spacing given by

$$d' = (1 + \gamma)d \tag{2}$$

was considered with $\gamma = \pm.05$. We were not led to consider larger displacements due to the good agreement with experiment using the bulk spacing ($\gamma = 0$). The results for the relaxed surface geometries are compared in Figure 6 for the (00) and ($\overline{1}$0) beams at $\phi = 0°$, $\theta = 10°$. The calculated peak positons are also included in Tables 1 and 2. These comparisons indicate better overall agreement for the unrelaxed structure ($\gamma = 0$). Both the contracted and expanded geometries fail to reproduce experimental peaks which are reproduced by the unrelaxed geometry. We note the clear failure of the $\gamma = \pm.05$ cases to correctly describe the 75 - 100 eV structure in the (00) beam. The expanded geometry gives a slight improvement in the relative magnitudes of the doublet peaks at 46 and 65 eV in the (00) beam but gives a less satisfactory description of the ($\overline{1}$0) beam features. Conversely, the contracted geometry case gives the best description of the peak shapes in the ($\overline{1}$0) data but gives by far the worst description of the (00) beam data. As noted in Tables 1 and 2, the unrelaxed surface geometry also gives noticeably better agreement in peak positions for both the specular and non-specular beams for the data analyzed. One may, of course, legitimately argue that the peak positions for the relaxed surface structures could be improved by a change in the inner potential $V_o$ of a few electron volts. Indeed, the tabulated results indicate that a systematic shift of $V_o$ in opposite directions will improve the average agreement in peak positions for the $\gamma = \pm.05$ cases. This is consistent with physical considerations which suggest that the expanded (contracted) geometry should give peak positions systematically lower (higher) than the unrelaxed case. As discussed above, the relaxed surface geometries fail to adequately reproduce important spectral features which the unrelaxed geometry describes well. We feel these results are compelling evidence that the outer layer spacing of the Pt(111) planes is equal to the bulk value to within 5%. A refinement in the model would be an expansion or contraction of the second layer spacing. Simple physical considerations would suggest that this effect would be quite small, and we have therefore not considered this case.

## ACKNOWLEDGMENTS

The authors are grateful to Dr. O. Krogh Andersen for his assistance in providing us with tabulated values of the platinum potential used in Reference 16. We also wish to thank Mr. Peter Stair for useful discussions with regard to the experimental data.

This work was carried out under the auspices of the U.S. Atomic Energy Commission.

## REFERENCES

1. P. C. Stair, T. J. Kaminska, L. L. Kesmodel, and G. A. Somorjai, preceding paper.
2. D. W. Jepsen, P. M. Marcus, and F. Jona, Phys. Rev. Lett. 26, 1365 (1971); Phys. Rev. B 5, 3933 (1972); Phys. Rev. B 6, 3684 (1972).
3. G. E. Laramore and C. B. Duke, Phys. Rev. B 5, 267 (1972).
4. S. Y. Tong, T. N. Rhodin, and R. H. Tait, Phys. Rev. B 8, 421 (1973); Phys. Rev. B 8, 430 (1973).
5. M. R. Martin and G. A. Somorjai, Phys. Rev. B 7, 3607 (1973).
6. G. E. Laramore, Phys. Rev. B 8, 515 (1973).
7. S. Y. Tong and L. L. Kesmodel, Phys. Rev. B 8, 3753 (1973).
8. J. E. Demuth, D. W. Jepsen, and P. M. Marcus, in Proc. Seventh LEED Meeting, San Diego, California, March 1973; Bull. Am. Phys. Soc. 18 (1973).
9. G. Capart, Surf. Sci. 26, 429 (1971).
10. G. E. Laramore, Phys. Rev. B 9, 1204 (1974).
11. J. B. Pendry, J. Phys. C 4, 2514 (1971).
12. D. W. Jepsen, P. M. Marcus, and F. Jona, Phys. Rev. B 8, 5523 (1973).
13. J. L. Beeby, J. Phys. C 1, 82 (1968).
14. C. B. Duke and C. W. Tucker, Jr., Surf. Sci. 15, 231 (1969).
15. C. B. Duke and G. E. Laramore, Phys. Rev. B 2, 4765 (1970).
16. O. K. Andersen and A. R. Mackintosh, Solid State Commun. 6, 285 (1968); O. K. Andersen, Phys. Rev. B 2, 883 (1970).
17. J. C. Slater, Phys. Rev. 81, 385 (1951).
18. G. A. Somorjai and H. H. Farrell, Advan. Chem. Phys. 20, 215 (1972).
19. M. B. Webb and M. G. Lagally, Solid State Phys. 28, 301 (1973).

20. The value of the (polycrystalline) platinum work function of 5.4 eV is taken from thermionic emission results from R. O. Jenkins and W. G. Trodden, Electron and Ion Emission from Solids, (Dover, New York, 1967). Measured values range from 5.3-5.8 eV. See, for example, R. G. Wilson, J. Appl. Phys. 37, 2261 (1966); R. Bouwman, H. P. van Keulen, and W. M. H. Sachtler, Ber. Bunsenges. Physik. Chem. 74, 198 (1970).
21. See, for example, E. Merzbacher, Quantum Mechanics, (Wiley, New York, 1967), p. 233.
22. See, for example, G. A. Somorjai, Principles of Surface Chemistry (Prentice-Hall, New Jersey, 1972), p. 99.
23. F. Jona, I.B.M. J. Res. Dev. 14, 444 (1970).

TABLE 1

PLATINUM (111) PEAK POSITIONS: (00) BEAM (Values in Electron Volts)

| Angle | Exp. (Ref. 1) | Theory | Δ | Remarks |
|---|---|---|---|---|
| θ=4° ϕ=0° | 22 | $16^a$ | -6 | Exp. position uncertain |
| | 47 | $48^a$ | +1 | |
| | 72 | $70^a$ | -2 | shoulder |
| | 92 | $91^a$ | -1 | shoulder |
| | 103 | $101^a$ | -2 | |
| | | | $\lvert\bar{\Delta}\rvert=2.4^a$ | Avg. based on 5 peaks |
| θ=10° ϕ=0° | <20 | $17^a$ | | Exp. position undetermined |
| | | $16^b$ | | |
| | | $18^a$ | | |
| | 34 | $34^a$ | 0 | |
| | | $34^b$ | 0 | |
| | | $35^c$ | +1 | Weak shoulder in theory |
| | 46 | $51^a$ | +5 | |
| | | $49^b$ | +3 | |
| | | $54^c$ | +8 | Shoulder in theory |
| | 65 | $64^a$ | -1 | |
| | | $63^b$ | -2 | |
| | | $64^c$ | -1 | |

Table 1, cont'd.

| | | | | |
|---|---|---|---|---|
| | 78 | $78^a$ | 0 | |
| | | $75^b$ | -3 | |
| | | $81^c$ | +3 | |
| | 91 | $90^a$ | -1 | Shoulder |
| | | $90^b$ | -1 | Major peak in theory |
| | | $(\ )^c$ | | Peak absent in theory |
| | 98 | $98^a$ | 0 | |
| | | $(\ )^b$ | | Peak absent in theory |
| | | $100(+)^c$ | | |
| | | | $\lvert\bar{\Delta}\rvert=1.2^a$ | Avg.based on 6 peaks |
| | | | $\lvert\bar{\Delta}\rvert=1.8^b$ | Avg. based on 5 peaks |
| | | | $\lvert\bar{\Delta}\rvert=3.3^c$ | Avg. based on 4 peaks |
| $\theta=16°$ $\phi=4.3°$ | <20 | $16^a$ | | Exp. position undetermined. |
| | 49 | $51^a$ | +2 | Major peak of doublet in exp.<br>Shoulder in theory. |
| | 57 | $57^a$ | 0 | Minor peak of doublet in exp.<br>Major peak in theory. |
| | 68 | $69^a$ | +1 | Minor peak of doublet<br>Shoulder in theory. |
| | 77 | $76^a$ | -1 | Major peak of doublet |
| | 101 | $103^a$ | +2 | |
| | | | $\lvert\bar{\Delta}\rvert=1.2^a$ | Avg. based on 5 peaks |

Average for (00) Beam based on analysis of 16 peaks:

$|\bar{\Delta}| = 1.6^a$

---

[a] Theory with bulk interlayer spacing for Pt(111) planes ($\gamma=0$).

[b] Theory with 5% expansion of outer layer in direction normal to surface ($\gamma=0.05$)

[c] Theory with 5% contraction of outer layer in direction normal to surface ($\gamma=-0.05$).

## TABLE 2

PLATINUM (111) PEAK POSITIONS: NON-SPECULAR BEAMS (Values in Electron Volts)

| Beam | Angle | Exp.(Ref.1) | Theory | $\Delta$ | Remarks |
|---|---|---|---|---|---|
| $(\bar{1}0)$ | $\theta=4^\circ$ $\phi=0^\circ$ | 41 | 42[a] | +1 | |
| | | 60 | 61[a] | +1 | |
| $(\bar{1}0)$ | $\theta=10^\circ$ $\phi=0^\circ$ | 29 | 33[a] | +4 | |
| | | | 32[b] | +3 | |
| | | | 34[c] | +5 | |
| | | 47 | 48[a] | +1 | |
| | | | 47[b] | 0 | |
| | | | 49[c] | +2 | |
| | | 59 | 59[a] | 0 | |
| | | | 58[b] | -1 | |
| | | | 60[c] | +1 | |
| | | 68 | 68[a] | 0 | |
| | | | 65[b] | -3 | Shoulder in theory |
| | | | 68[c] | 0 | |
| $(\bar{1}0)$ | $\theta=16^\circ\phi=4.3^\circ$ | 29 | 31[a] | +2 | |
| | | 42 | 44[a] | +2 | |
| | | | | $\lvert\bar{\Delta}\rvert=1.4$[a] | Avg.based on 8 peaks |
| | | | | $\lvert\bar{\Delta}\rvert=1.8$[b] | Avg.based on 4 peaks |
| | | | | $\lvert\bar{\Delta}\rvert=2.0$[c] | Avg.based on 4 peaks |

Table 2, cont'd.

| | | | | | |
|---|---|---|---|---|---|
| (01) | $\theta=\phi=0°$ | <44 | 40[a] | | Exp.position undetermined. |
| | | 55 | ( )[a] | | Shoulder peak in exp. Peak absent except as broad shoulder in theory |
| | | 73 | 73[a] | 0 | |
| | | 82 | 82[a] | 0 | |
| (10) | $\theta=\phi=0°$ | <46 | 44[a] | | Exp.position undetermined |
| | | 52 | ( )[a] | | Narrow shoulder peak i<br>exp.<br>Peak absent in theory |
| | | 60 | 62[a] | +2 | |
| | | 79 | 86[a] | +7 | Broad flat peak |
| | | | | $\lvert\bar{\Delta}\rvert=2.3$[a] | Avg.based on 4 peaks |

Average for non-specular beams based on analysis of 12 peaks:

$\lvert\bar{\Delta}\rvert = 1.7$[a]

---

[a] Theory with bulk interlayer spacing for Pt(111) planes ($\gamma=0$)

[b] Theory with 5% expansion of outer layer in direction normal to surface ($\gamma=0.05$)

[c] Theory with 5% contraction of outer layer in direction normal to surface ($\gamma=-0.05$)

# FIGURE CAPTIONS

Fig. 1. Platinum phase shifts in radians for the model potential used in the band structure calculation of Reference 16. The energy scale is referred relative to the constant value of the potential between muffin-tin spheres.

Fig. 2. Modulus of the platinum atomic scattering factor vs. scattering angle at 100 eV above the vacuum level as calculated from the model potential.

Fig. 3. Schematic illustrating (a) the platinum(111) diffraction pattern as viewed on the fluorescent screen and (b) the orientation of the atoms in the surface unit cell with respect to the diffraction pattern. The labels A, B, and C refer to atoms in the first, second, and third atomic layers from the surface (the stacking sequence is ABC ABC ...). The diagram is to be regarded from the perspective of looking "through" the crystal sample (target) towards the diffraction pattern; i.e., the topmost atomic layer is farthest from the observer. The electron beam is incident horizontally from the left. The beam labelling and designation of azimuthal orientations follow the convention of Jona (Reference 23).

Fig. 4. Comparisons of theory and experiment for intensity-energy profiles from Pt(111) at room temperature for (a) the (00) beam and (b) the $(\overline{1}0)$ beam at three angles of incidence. The vertical scales are of relative intensity in arbitrary units and are not necessarily compatible from one curve to the next. The theoretical results were calculated on the assumption of the bulk interplanar spacing for all atomic layers parallel to the surface and an inner potential $V_o$ = 14.3 eV. The experimental data is taken from Reference 1.

Fig. Capt., cont'd.

Fig. 5. Comparisons of theory and experiment for intensity-energy profiles from Pt(111) at room temperature for (a) the $(01) = (\bar{1}0) = (1\bar{1})$ beam and (b) the $(10) = (0\bar{1}) = (\bar{1}1)$ beam at normal incidence. Other conditions are as in Figure 4.

Fig. 6. Effect of a small change in the lattice spacing of the topmost atomic layer in the direction perpendicular to the surface on the calculated intensity profiles. The designation $\gamma = 0$ corresponds to a spacing equal to the bulk value and $\gamma = .05$ and $\gamma = -.05$ correspond to 5% expansion and contraction, respectively, relative to the bulk spacing. The vertical scales are relative intensities in arbitrary units and are not necessarily compatible from one curve to the next. The comparisons are made at $\phi = 0°$, $\theta = 10°$ for (a) the (00) beam and (b) the $(\bar{1}0)$ beam. The experimental data is taken from Reference 1.

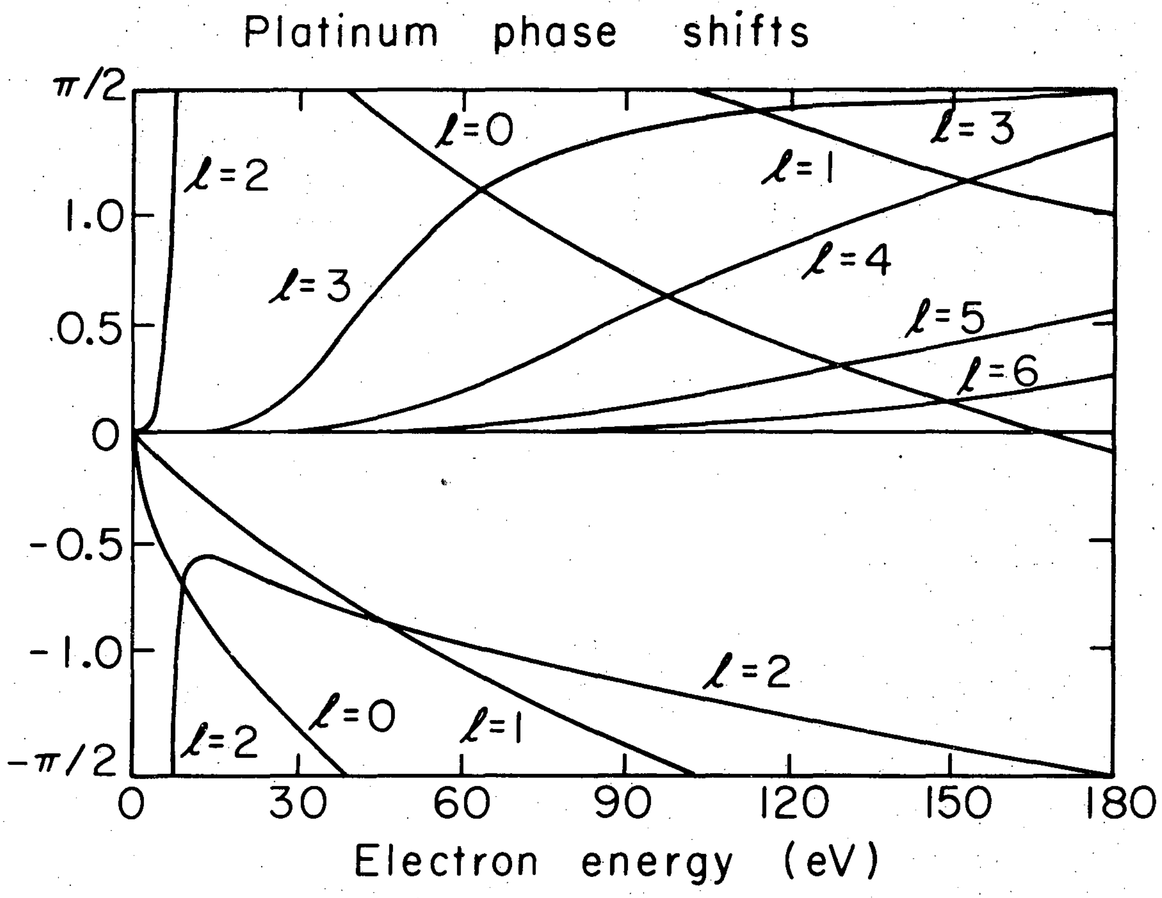

XBL 748-3881

Fig. 1

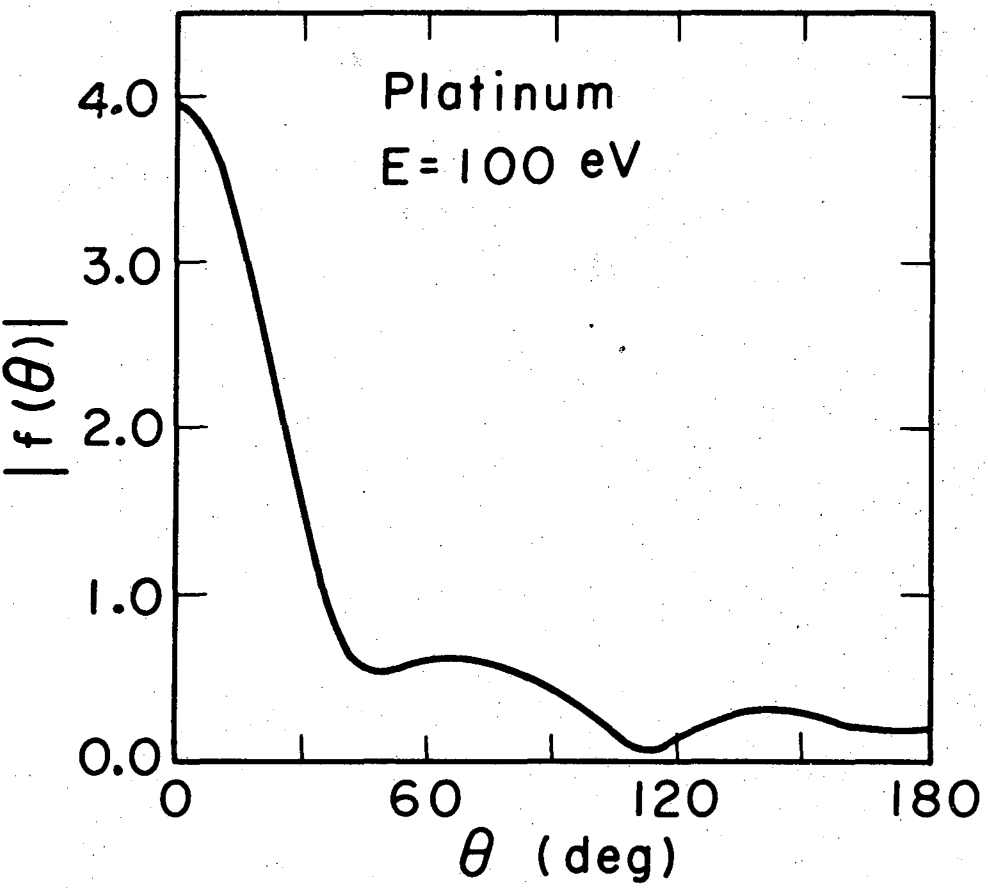

XBL748-3882

Fig. 2

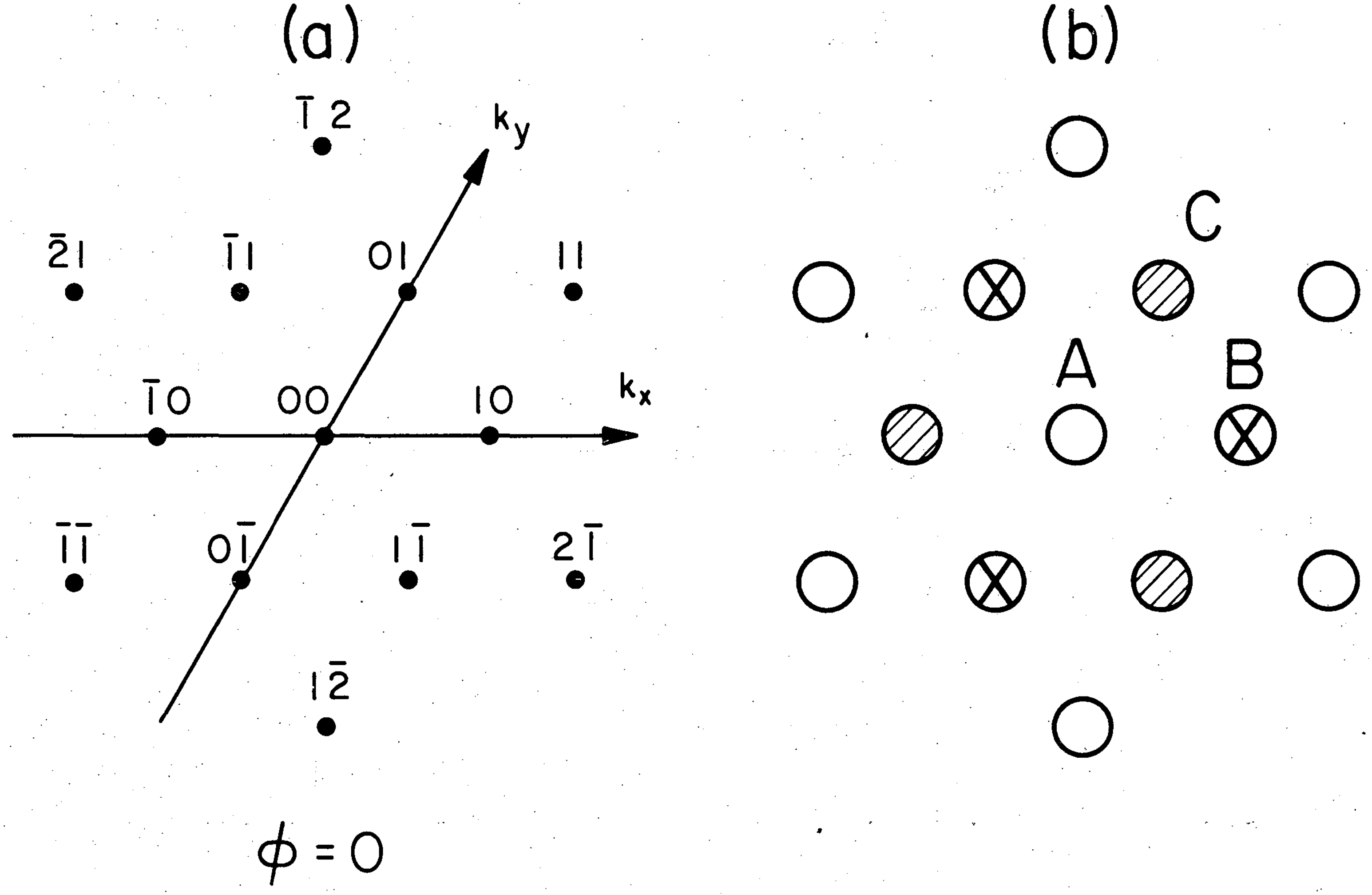

XBL748-3878

Fig. 3

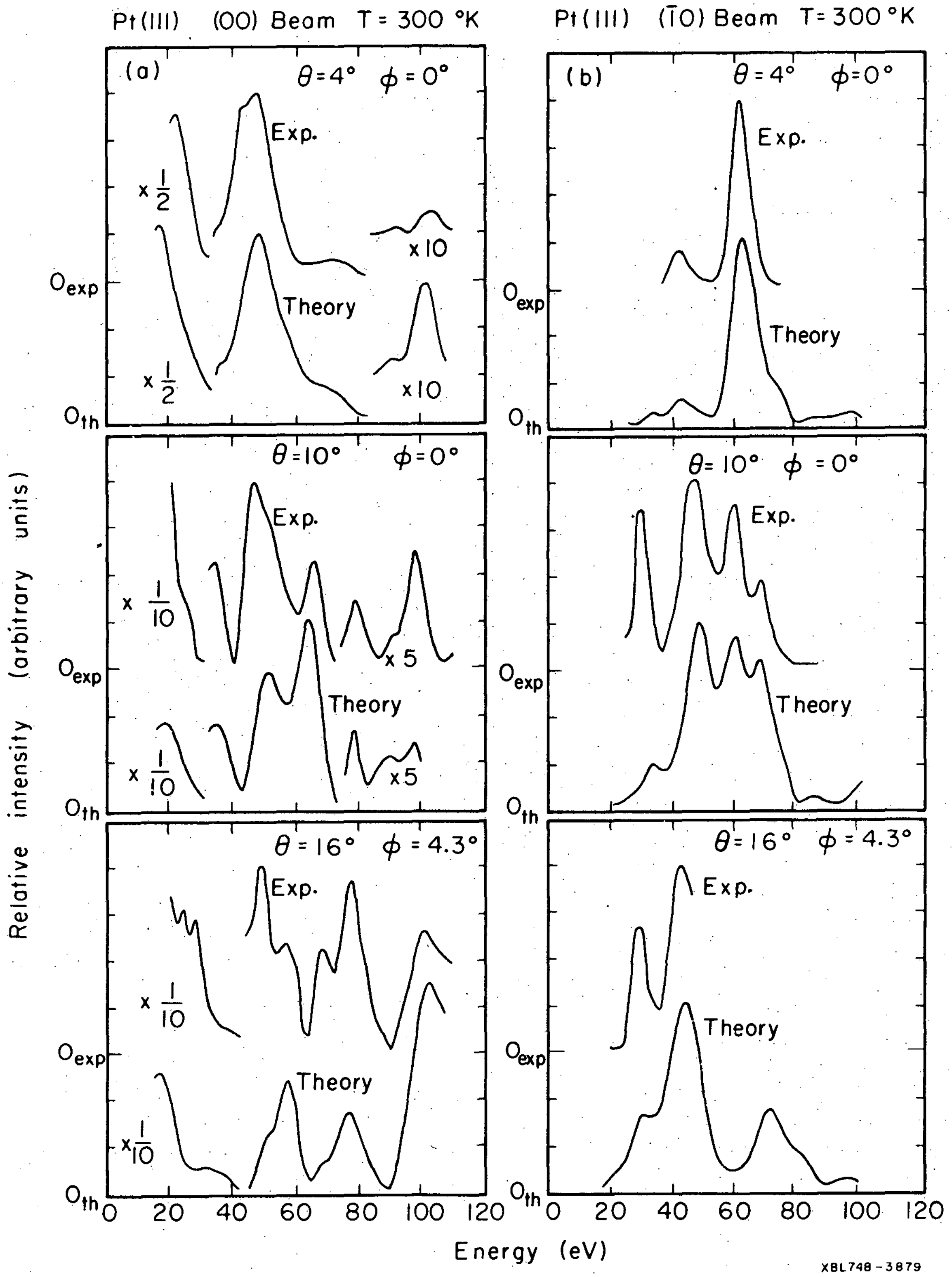
Pt(111) (00) Beam T = 300 °K
Pt(111) (1̄0) Beam T = 300 °K
(a)
(b)
θ = 4° φ = 0°
θ = 10° φ = 0°
θ = 16° φ = 4.3°
Exp.
Theory
x 1/2
x 10
x 1/10
x 5
0exp
0th
Relative intensity (arbitrary units)
0
20
40
60
80
100
120
Energy (eV)
XBL748-3879

Fig. 4

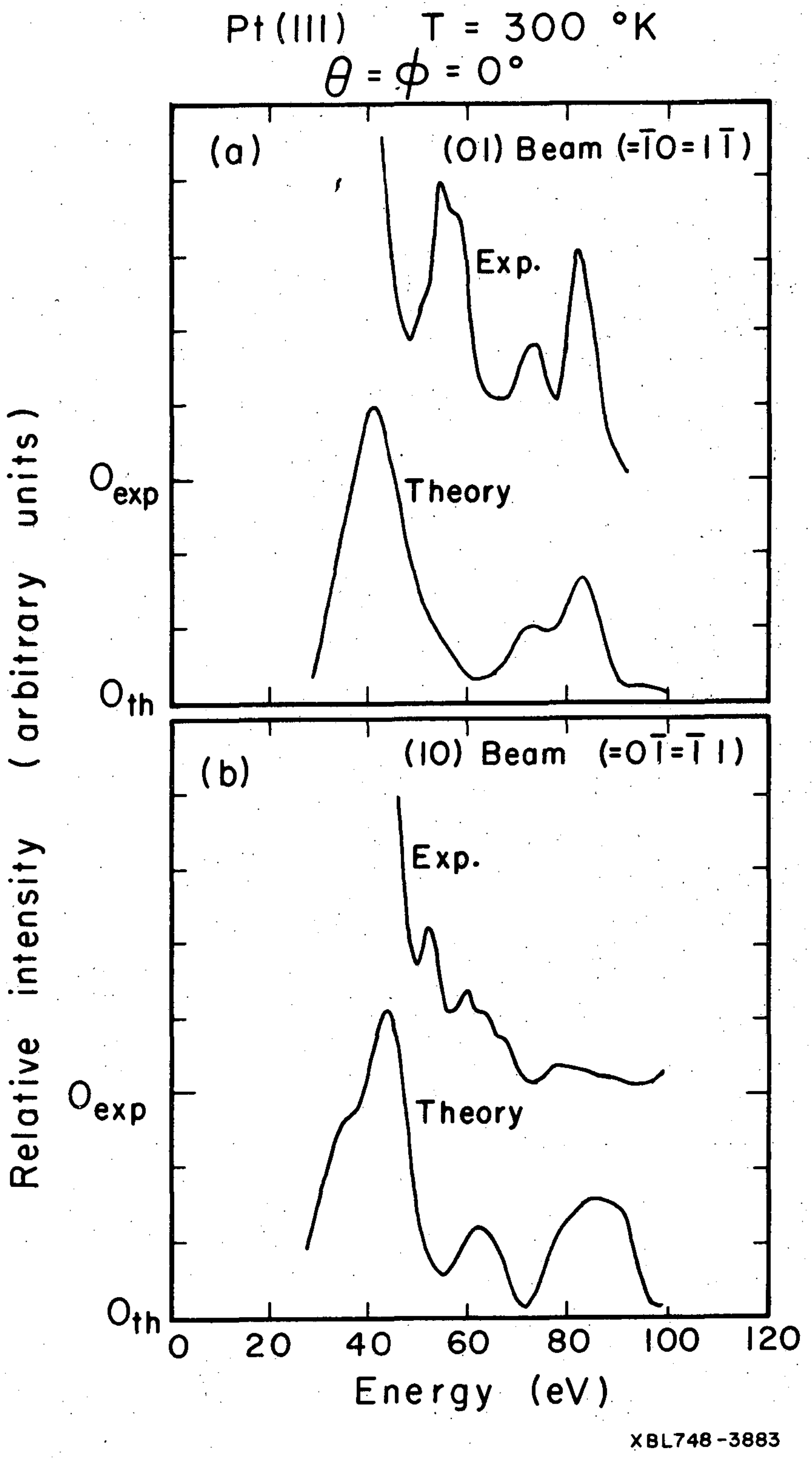
Pt(111) T = 300 °K
$\theta = \phi = 0°$
(a)
(01) Beam ($=\bar{1}0=1\bar{1}$)
Exp.
Theory
$0_{exp}$
$0_{th}$
(b)
(10) Beam ($=0\bar{1}=\bar{1}1$)
Exp.
Theory
$0_{exp}$
$0_{th}$
Relative intensity (arbitrary units)
0
20
40
60
80
100
120
Energy (eV)
XBL748-3883

Fig. 5

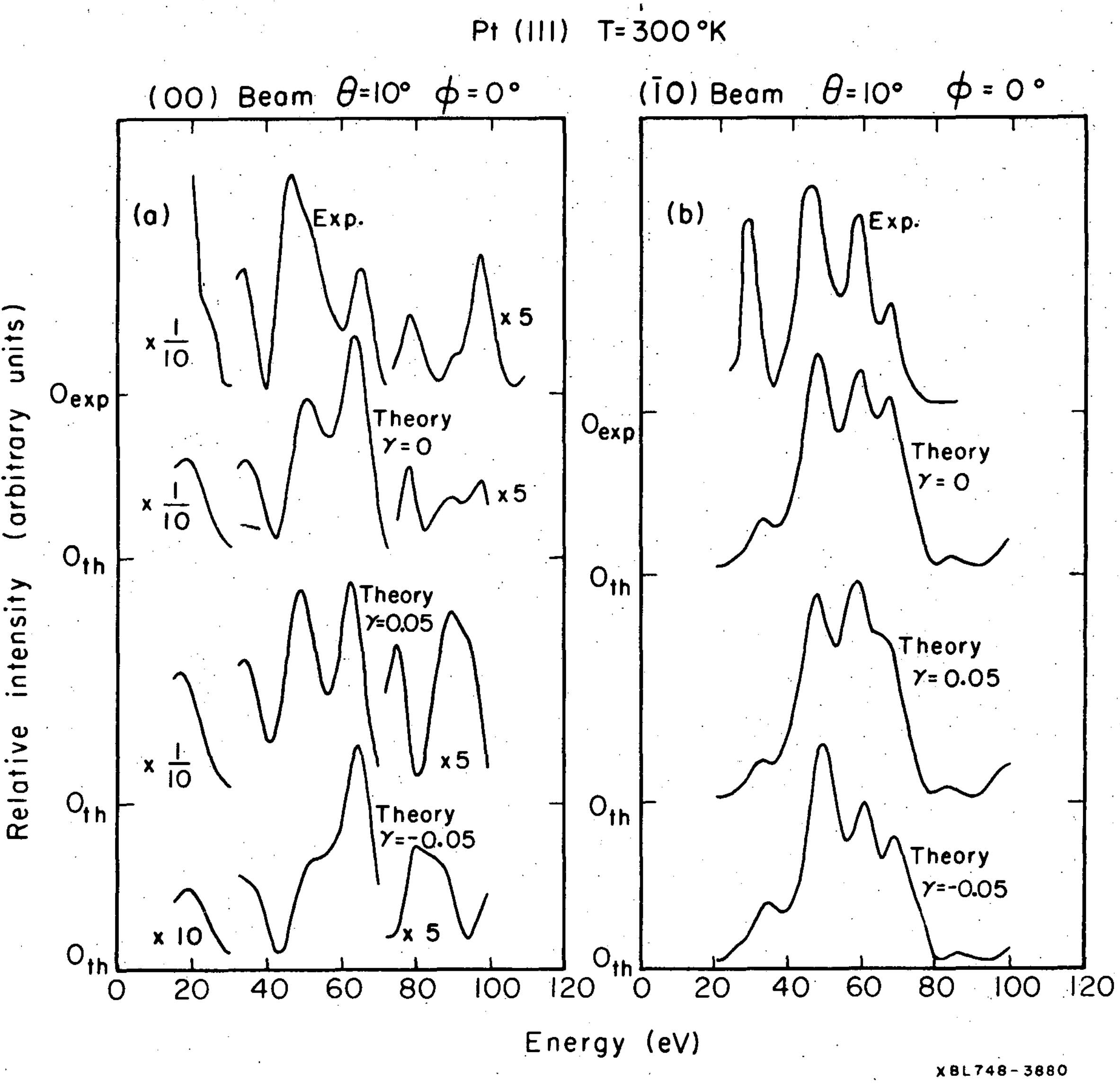
Pt (111) T=300°K
(00) Beam θ=10° φ=0°
($\bar{1}$0) Beam θ=10° φ=0°
(a)
(b)
Exp.
Theory γ=0
Theory γ=0.05
Theory γ=-0.05
x 1/10
x 5
x 10
$0_{exp}$
$0_{th}$
Relative intensity (arbitrary units)
Energy (eV)
0
20
40
60
80
100
120
XBL748-3880

Fig. 6

LEGAL NOTICE

*This report was prepared as an account of work sponsored by the United States Government. Neither the United States nor the United States Atomic Energy Commission, nor any of their employees, nor any of their contractors, subcontractors, or their employees, makes any warranty, express or implied, or assumes any legal liability or responsibility for the accuracy, completeness or usefulness of any information, apparatus, product or process disclosed, or represents that its use would not infringe privately owned rights.*

TECHNICAL INFORMATION DIVISION
LAWRENCE BERKELEY LABORATORY
UNIVERSITY OF CALIFORNIA
BERKELEY, CALIFORNIA 94720